Enthalpy of fusion prediction for the economic optimisation of salt based latent heat thermal energy stores

Heinrich Badenhorst[a*], Thomas Böhmer[b]

[a] *The University of Manchester, School of Chemical Engineering & Analytical Science, The Mill,*
Sackville Street, Manchester, United Kingdom, M1 3AL
[b] *University of Pretoria, Department of Chemical Engineering, Lynnwood Road, Pretoria, South*
Africa, 0083

Highlights

- Thermodynamic modelling of enthalpy of fusion using entropy and enthalpy approaches.
- Best practical option found to be ideal liquid, immiscible solid and entropic approach.
- Generalised to require only melting temperature measurements.
- Screened all ternary combinations of 35 salts resulting in achieved storage cost of 1.8 $/MJ.
- Demonstrated that the use of non-eutectic slurries can reduce cost to below 0.045 $/MJ.

Abstract

Thermal energy storage represents a cost-effective means of integrating variable, renewable resources into the energy mix. The utilisation of latent heat in addition to sensible can reduce capital costs. To accurately screen the numerous possible ionic salts, accurate enthalpy of fusion predictions are essential. Three possible modelling approaches were considered: enthalpic, regular solution entropic and rigorous entropic. These approaches were combined with different techniques to represent the enthalpy of mixing and the temperature-composition dependence.

Ultimately it was found that disregarding the entropy of mixing and assuming an ideal liquid phase, combined with an immiscible solid phase resulted in adequate predictions of the experimental data. The approach can be used to rapidly screen a wide range of components using only pure component properties. It can be further generalised to require only melting temperatures through the use of a modified

---

[*] Corresponding author. Tel: +44 (0)161 306 4387. E–mail: heinrich.badenhorst@manchester.ac.uk

“Richard’s Rule”. The method was used to economically compare binary and ternary combinations over the range of 290-565 ºC.

The analysis indicated that ternary eutectic mixtures can achieve storage costs using fine chemicals of around 0.18 ± 0.045 \$/kJ, with bulk materials conservatively estimated to cost more than 100 times less at ~1.8 \$/MJ. This assumes that storage is achieved through a combination of latent and sensible heat. A set of eight suitable salt candidates were identified that require detailed thermal studies. Lastly it was demonstrated that the use of non-eutectic mixtures, using for example $LiNO_3$ and KCl, may hold the key to bulk storage costs as low as 0.045 \$/MJ, if the issues facing practical implementation can be mitigated.

Keywords: enthalpy of fusion, thermodynamic model, thermal energy storage

1. Introduction

To improve the long term sustainability of energy supplies, renewable resources are being increasingly incorporated into the electricity grid. However, significant issues hindering widespread implementation are the variability of renewable supplies, in conjunction with supply-demand mismatches [1-3]. Thermal energy storage (TES) systems can be used to mitigate these issues by storing heat during times of excess supply and discharging when demand is at its peak. Despite the fact that TES has already been implemented on industrial scale [4,5], these systems are not yet fully cost-optimised. The current sensible heat based implementations comprise roughly 30% of the total capital expenditure for concentrated solar power plants [6-8]. If this cost could be reduced it may hold the key to enabling pervasive integration of stable, renewable energy resources.

In an effort to increase storage density and thereby bring down costs, systems which incorporate phase transitions are being explored. Latent heat thermal energy storage (LHTES) incorporates the enthalpy of fusion in addition to sensible heat, in order to increase the energy stored per unit mass (kJ/kg). However, simply maximising the energy density does not guarantee economical optimality since the material under consideration may be too expensive (\$/kg). Thus it is necessary to consider both the energy density and the cost, or simply the cost per unit energy stored (\$/kJ), in order to find the optimal storage material.

From a power generation perspective it would be preferred if the stored energy could be recovered at a roughly constant temperature, thereby mitigating complex heat integration and pinch considerations [9]. The required temperature will vary widely depending on the power block requirements, as influenced by the type and configuration of the turbine. Pure component phase transition occurs at a specific temperature, thus it is necessary to match the most economical option to a given application temperature. From a thermodynamic perspective higher temperatures result in higher overall efficiencies. Thus in the long term, the objective is to move to power blocks which are capable of operating at progressively higher temperatures.

An alternative solution to the use of pure compounds is the option of multicomponent mixtures. For high temperature storage, ionic salts have been identified as suitable candidates [10-14]. Salt mixtures tend to form low melting eutectics at one or more compositions. Eutectic solutions behave much like pure components, with a single, fixed phase transition temperature at which the entire mixture melts and freezes. At compositions other than the eutectic, freezing will either occur as a pure component or a multicomponent phase. This component or phase remains in equilibrium with the melt, from its initial melting point up to the eutectic point. When this temperature is reached the remaining material will solidify at the eutectic composition. Thus this process creates a multi-phase solid system, which may lead to incongruent melting and component segregation issues. However, provided there is some mixing when the system is completely molten, this may prove to be inconsequential in practice, thus both eutectic and non-eutectic mixtures should be considered.

The objective of the investigation is to identify a set of salts which are the most likely to minimise energy storage cost over the range of temperatures of interest to industrial scale energy storage for power generation. This will form the starting point for detailed future studies of their thermal properties. However, in order to fully explore the feasibility of a set of candidate materials and their mixtures, accurate prediction of the enthalpy of fusion is a necessity. As pointed out by a recent review [15], very little work has been done on the estimation of the mixture heat of fusion, using pure component and mixture properties.

Prior work in this area has focused almost exclusively on the ability to predict the phase diagram [16-18], i.e. composition as a function of temperature. In contrast, the current investigation explores the influence of increasing non-ideality on the predicted enthalpy of fusion for both eutectic and non-eutectic mixtures. Both enthalpic and entropic approaches are considered as starting points for the derivation of the model equations. The aim is to determine the minimum number of parameters required for the satisfactory estimation of the enthalpy of fusion, at any composition. In addition, the prediction of the melt composition and the melting temperature are also examined since, in some models, these are required inputs for the enthalpy estimation. The predictions are compared to multiple, experimentally measured binary systems across the whole composition range.

To further generalise the work an attempt is made to estimate the pure component enthalpies of fusion. The inference is based on the melting temperature, a property which is easier to measure using a variety of techniques and at a higher confidence than typically associated with enthalpy measurements. This allows the prior approach to be applied to components for which accurate enthalpy of fusion data is not available. The different estimation methods are further validated against the measured enthalpies of more than 20, binary, salt eutectics. This establishes the extent to which the estimate is degraded by a lack of measured enthalpy data.

The most suitable enthalpy estimate was then used to evaluate a set of thirty five ionic salts for the cost optimisation of LHTES as a function of storage temperature. This process constitutes a preliminary screening to identify the most attractive candidates, as well as establishing the achievable energy storage cost. The investigation is limited to four halide salts (F, Cl, Br and I) in addition to the nitrates, carbonates and sulphates of three alkali metals (Li, Na and K) and two alkali earth metals (Mg and Ca). Thus a total of 35 salts have been screened. The analysis considers both eutectic and non-eutectic mixtures, across a wide temperature range, using between one and four components. The optimal candidates are identified at temperature intervals of 5 ºC across the range.

The obtained optima are compared to traditional, sensible heat options to quantify the competitive advantage of utilising LHTES. The proposed approach provides a framework for identifying and analysing potential LHTES candidates using first principles based prediction of the enthalpy of fusion and minimal measured parameters. This enables rapid screening of a very wide range of materials for which only limited data is available. The work aims to highlight which LHTES materials are the most economically attractive, in order to limit the number of compounds requiring detailed thermal analysis.

2. Theory

2.1. The enthalpic approach

Since enthalpy is a state quantity it is often convenient to estimate the value of a specific transition by considering a hypothetical closed cycle. The melting temperature of a mixture varies with composition, but the enthalpy of fusion of a mixture at a given melting temperature (including the eutectic melting temperature) should be quantifiable based on its respective components. To achieve this one possible cycle can be described as follows:

1) Two pure components in the solid phase are taken from the mixture melting temperature ($T_{m,mix}$) to their individual melting temperatures ($T_{m,i}$)
2) They undergo melting, represented by the pure component enthalpies of fusion of each ($\Delta H_{fus,i}$)
3) Both liquids are cooled to the mixture melting temperature and are mixed in the liquid phase, constituting an enthalpy change of mixing (ΔH_{mix})
4) The mixture is frozen, releasing the enthalpy of fusion of the mixture ($\Delta H_{fus,m}$)
5) The solid mixture is “unmixed”, reconstituting the individual solids at their starting temperatures and having an associated enthalpy change of mixing (ΔH_{unmix})

This cycle can be represented mathematically by:

$$0 = \sum_{i} x_i \left(\int_{T_{m,mix}}^{T_{m,i}} Cp_{s,i} dT + \Delta H_{fus,i} + \int_{T_{m,i}}^{T_{m,mix}} Cp_{l,i} dT \right) + \Delta H_{mix,\ liquid} - \Delta H_{fus,m} + \Delta H_{unmix,\ solid} \quad (1)$$

The final step is impossible to perform in practice; however it is conceptually possible in reverse. It may be assumed that the solid mixture (after freezing) was ground into a powder as part of this process. Then the reverse step hypothetically represents the mechanical mixing of two solid powders. The energy associated with such a path would depend on a variety of factors which determine the extent to which ordering is developed in the cooling mixture. Under conditions of rapid cooling the random nature of the liquid phase will be maintained, as opposed to slow cooling which could enable the formation of a more structured lattice.

Practically, the energy required to mill a brittle material such as a salt into a powder is comparatively low and there is no energy change associated with the mixing of two pure powders. Thus it is expected that the final term in equation (1) may be considered negligible compared to the others. Additionally, since the mixture melting temperatures are comparatively close to the melting temperature of the individual constituents and the heat capacities of solid and liquid salts are usually fairly similar, the sensible heat terms may also be omitted to yield:

$$\Delta \mathrm{H}_{\mathrm{fus,m}} = \sum_{\mathrm{i}} \mathrm{x_i} \Delta \mathrm{H}_{\mathrm{fus,i}} + \Delta \mathrm{H}_{\mathrm{mix}} \quad (2)$$

This essentially constitutes the definition of the enthalpy of mixing, applied to multicomponent fusion as a type of mixing process. In the case of an ideal mixture the enthalpy of mixing may be neglected which gives the equation proposed by Raud et al. [19] for the prediction of the enthalpy of fusion of a mixture.

2.2. The entropic approach

Entropy is also a state quantity; however using the third law of thermodynamics it is possible to obtain an absolute value for the entropy. Thus in order to obtain the entropy of a phase transition it is not necessary to consider a closed cycle. Instead the absolute entropy of the constituents as well as the mixture, can be calculated at a given temperature starting from zero entropy, i.e. zero Kelvin. Hence the following two cases can be considered equivalent, as proposed by Kosa et al. [20]:

A) The two pure component solids are heated from zero Kelvin to their individual melting points. They undergo phase transition and each is cooled to the mixture melting temperature. At this point they are mixed in the liquid phase, with an associated entropy change of mixing (ΔS_{mix})

B) A mixture of the components in the solid phase, is heated from zero Kelvin to the mixture melting temperature where it undergoes melting

These two processes are quantified mathematically by:

$$\sum_i x_i \left(\int_0^{T_{m,i}} \frac{Cp_{s,i}}{T} dT + \Delta S_{fus,i} + \int_{T_{m,i}}^{T_{m,mix}} \frac{Cp_{l,i}}{T} dT \right) + \Delta S_{mix} \quad (3)$$

$$\int_0^{T_{m,mix}} \frac{Cp_{s,m}}{T} dT + \Delta S_{fus,m} \quad (4)$$

By employing the Neumann-Kopp law to relate the heat capacity of the solid mixture to that of the individual components [20], the integrals from zero Kelvin up to the mixture melting point may be eliminated. Using this and equating these two expressions produces the equation derived by Kosa et al. [20]:

$$\Delta S_{fus,m} = \sum_i x_i \left(\int_{T_{m,mix}}^{T_{m,i}} \frac{Cp_{s,i}}{T} dT + \Delta S_{fus,i} + \int_{T_{m,i}}^{T_{m,mix}} \frac{Cp_{l,i}}{T} dT \right) + \Delta S_{mix} \quad (5)$$

As before, in the enthalpic approach, it may be assumed that the sensible heat terms are negligible. The thermodynamic Gibbs free energy is defined as [21]:

$$G \equiv H - TS \text{ and by implication } G^E = H^E - TS^E \quad (6)$$

For an equilibrium process, such as the transition from solid to liquid phase (at constant temperature, T_{fus}), the associated Gibbs free energy change is zero [22], thus in general:

$$\Delta S_{fus} = \frac{\Delta H_{fus}}{T_{fus}} \quad (7)$$

Similarly for the process of mixing (at constant temperature, T_{mixing}) it may be stated that:

$$\Delta S_{mix} = \frac{\Delta H_{mix} - \Delta G_{mix}}{T_{mixing}} \quad (8)$$

Based on fundamental considerations and the definitions of the appropriate quantities, the following two equations can be established [21]:

$$\frac{G^E}{RT} = \sum_i x_i \ln(\gamma_i) \quad (9)$$

$$\Delta G_{mix} = G^E + RT \sum_i x_i \ln(x_i) \quad (10)$$

Substituting equation (9) into (10) and the result back into (8) yields:

$$\Delta S_{mix} = \frac{\Delta H_{mix}}{T_{mixing}} - R \sum_i x_i \ln(\gamma_i x_i) \quad (11)$$

By substituting equations (7) and (11) into equation (5), entropy may be eliminated from the expression. Noting that in case A) it is stated that mixing occurs at the mixture melting temperature ($T_{m,mixture}$) and rearranging, one arrives at:

$$\Delta H_{fus,m} = T_{m,mixture} \sum_i x_i \left(\frac{\Delta H_{fus,i}}{T_{m,i}} - R \ln(\gamma_i x_i) \right) + \Delta H_{mix} \quad (12)$$

The derivation has been based on the assumption that freezing occurs at the mixture melting temperature. For freezing at the eutectic temperature this is fundamentally consistent. However, even for a simple eutectic the real situation is not as straightforward, as indicated in Figure 1.

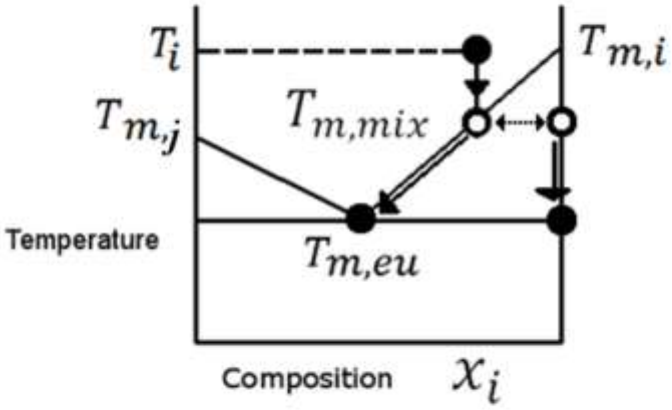

Fig. 1: Behaviour of a simple eutectic cooled from T_i at composition x_i

During freezing the system moves from the initial mixture melting temperature to the eutectic temperature, beyond which the mixture is fully solidified. Since the temperature range is comparatively small, this effect is usually considered negligible and thus the approach is applied to all mixtures.

In traditional thermodynamics three solution models are commonly used: ideal, regular and real [23]. For an ideal solution the excess entropy of mixing is zero and hence [23]:

$$\Delta S_{mix} = \Delta S_{mix}^{ideal} = -R\sum_i x_i \ln(x_i) \quad (13)$$

For both regular and real solutions the entropy of mixing is also assumed to be ideal. Thus in all cases equation (11) is effectively replaced by (13), resulting in a simplified form of equation (12):

$$\Delta H_{fus,m} = T_{m,mix}\sum_i x_i\left(\frac{\Delta H_{fus,i}}{T_{m,i}} - R\ln(x_i)\right) \quad (14)$$

Expressions (2) and (14) for calculating the enthalpy of fusion have also presented by Misra and Whittenberger [24].

2.3. Phase behaviour of ionic salts

The simple eutectic illustrated in Figure 1 represents a system where the solid phase is considered immiscible. This means a pure salt is in equilibrium with the molten salt mixture. Thus during melting/freezing only one component is transferred between these two phases. A slightly more complex behaviour, more typically found in these mixtures, is demonstrated in Figure 2.

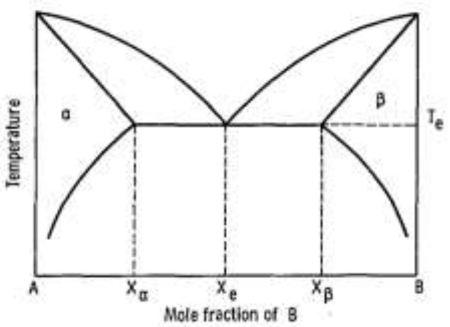

Fig. 2: Behaviour of a complex eutectic [24]

This is known as having terminal solid solutions and implies that the liquid melt is in equilibrium with multicomponent solid phases, α and β, as opposed to the pure components. Hence in this case the melting/freezing process involves the simultaneous transfer of both components (for a binary) between the phases. In these cases simply approximating the liquidus line as a straight-line, as in the case of the simple eutectic, may provide a sufficiently accurate estimate of the initial melting point. Even more complex scenarios exist where the system may exhibit multiple eutectics as shown in Figure 3.

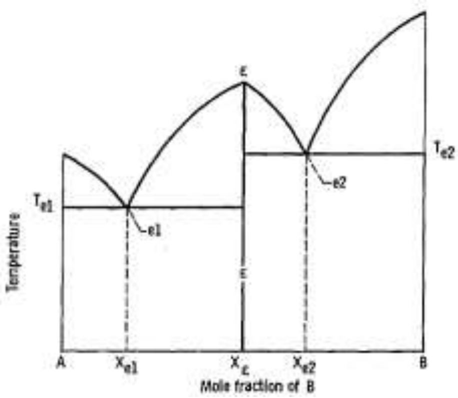

Fig. 3: Multi-eutectic behaviour [24]

For these very complex cases detailed modelling of the phase behaviour is required, specifically information regarding the intermediate phase/compound. If this is known the diagram can be split into segments and each eutectic modelled as before. However, during screening of a wide variety of components, it is likely that this information will not be available. The current approach will at least give a very rough approximation of the temperature range and expected enthalpy of fusion for estimating the storage cost during initial selection. This estimate can then be refined if complex behaviour is found for the system exhibiting the lowest cost.

2.4. The enthalpy of mixing

For an ideal solution the enthalpy of mixing is assumed to be zero, whereas in the regular and real solution models it is not. For the regular solution model the enthalpy of mixing is assumed to be a function of composition only, whereas for real solutions it is additionally a function of temperature [23]. Since this investigation is only concerned with the behaviour in a relatively narrow range around the melting/freezing temperature, real solution behaviour will not be considered. Since the entropy of mixing is ideal in all cases, the excess entropy is zero. This implies the excess Gibbs energy is equal to the excess enthalpy using (6). Furthermore, since the excess enthalpy is by definition equal to the enthalpy of mixing, the result is that, from equation (9):

$$\frac{G^E}{RT} = \frac{H^E}{RT} = \frac{\Delta H_{mix}}{RT} = \sum_i x_i \ln(\gamma_i) \quad (15)$$

Thus any one of the following options is a valid solution for determining the enthalpy of mixing:

1) Specify a model for the excess Gibbs energy, for example the Wilson [25] or UNIQUAC [26] expressions
2) Specify an empirical expression for the enthalpy of mixing, as done by Kleppa and Hersh [27]
3) Determine the activity coefficients directly from the phase diagram, as indicated by Misra and Whittenberger [24]

This list is not exhaustive but serves to classify the variety of approaches found in literature. For option 1) the Wilson equation is often used and is expressed as:

$$\frac{G^E}{RT} = -\sum_i x_i \ln\left(\sum_j x_j \Lambda_{ij}\right) \quad (16)$$

The binary model has two parameters, Λ_{ij} and Λ_{ji}, which can either be found in literature or determined using the eutectic information if available. In option 2) the expression for the enthalpy of mixing is usually derived from experimental measurements and has the general form for binaries [27]:

$$\Delta H_{mix} = x_i(1 - x_i)[a + bx_i + cx_i(1 - x_i)] \quad (17)$$

Either of these approaches can be used to specify the enthalpy of mixing in equation (2) and (12). The third option requires complete knowledge of the phase diagram, which is unlikely to be available during preliminary investigations and hence this option is not considered in this study.

2.5. Temperature dependence on composition

Equation (2) is unique in the sense that if the enthalpy of mixing is specified, it requires no additional information other than the enthalpies of fusion of the pure components. For equations (12) and (14), using either an ideal or non-ideal enthalpy of mixing, an additional expression is required which gives the mixture melting temperature as a function of composition. To obtain this, an expression for phase equilibrium, at constant temperature and pressure, is conventionally used [21, 22]:

$$\hat{f}_i^l = \hat{f}_i^s \quad (18)$$

Where $\hat{f}_i^l$ is the fugacity of species i in the liquid solution and the superscript s represents the solid solution. The expression can be reformulated using the fugacities of the pure components and the activity coefficients:

$$x_i^l \gamma_i^l f_i^l = x_i^s \gamma_i^s f_i^s \quad (19)$$

The pure component fugacities can be related to the Gibbs free energy and in turn to the enthalpy, which can be integrated to yield [21]:

$$\psi_i \equiv {f_i^s}\Big/{f_i^l} = exp\left[\frac{\Delta H_{fus,i}}{RT_{m,i}}\left(\frac{T-T_{m,i}}{T}\right)\right] \quad (20)$$

In the simplest case, the assumptions are made that there is complete immiscibility for all species in the solid state, i.e. $x_i^s \gamma_i^s = 1$ and ideal-solution behaviour in the liquid state $\gamma_i^l = 1$. This leads to the simple eutectic behaviour demonstrated in Figure 1. The resulting expression for composition as a function of temperature is also called the Schröder or Schröder-van Laar equation [22]. This expression fully specifies the temperature-composition relationship using only the pure component melting points and enthalpies of fusion. In this case the equilibrium curve between solid and liquid is a straight line. Curvature can be taken into account, to a certain extent, by assuming non-ideal behaviour in the liquid phase ($\gamma_i^l \neq 1$) and retaining immiscibility in the solid phase. In this case the conventional expression for the activity coefficient can be used as given by [21]:

$$\ln \gamma_i = \left[\frac{\partial(nG^E/RT)}{\partial n_i}\right]_{T,P,n_j} \quad (21)$$

From equation (15) the excess Gibbs energy and the enthalpy of mixing are equivalent. Thus either a modelled expression (for G^E) or an experimental expression for the enthalpy of mixing can be used to determine the activity coefficient. Finally, by considering non-ideality in both the solid and liquid phases ($\gamma_i^l \neq 1$, $\gamma_i^s \neq 1$), the more complex behaviour exhibited in Figure 2 can be represented. However, in this case the prior expression (21) can no longer be used to determine the activity coefficients since it requires that all species, other than the one under consideration remain constant. For an immiscible solid phase this is the case but as mentioned, in the presence of terminal solid solutions, both components transfer between phases during phase transition. For a regular solution ($S^E = 0$), the partial molar enthalpy of mixing can be alternatively represented as [23]:

$$\ln \gamma_i = \Delta \bar{G}_i^E = \Delta \bar{H}_i^{mix} = \Delta H_{mix} + (1 - x_i)\frac{d\Delta H_{mix}}{dx_i} \quad (22)$$

Using this expression the activity coefficients can be found for both the solid and liquid phases, provided an expression is available for the enthalpy of mixing for *both liquid and solid*. The former was experimentally determined by Kleppa [28] for various salts. The latter is provided by Kramer and Wilson [29] and the current approach is equivalent to their alternative expression for the transition, using Gibbs free energy directly, expressed as:

$$\Delta G_i = 0 = \Delta H_{fus,i} - T\Delta S_{fus,i} + \left(\Delta \bar{H}_i^{mix} - T\Delta \bar{S}_i^{mix}\right)^{liquid} - \left(\Delta \bar{H}_i^{mix} - T\Delta \bar{S}_i^{mix}\right)^{solid} \quad (23)$$

Depending on the available information a variety of options exist for specifying the mixture enthalpy of fusion, the enthalpy of mixing and the temperature-composition dependence. A range of combinations are explored in the following sections, in order to determine the least information required for an acceptable representation.

3. Methods and calculations

3.1. Solution models

Based on the prior theoretical analysis the following progressively less ideal options for calculating the enthalpy of fusion exist:

1) Enthalpic approach, i.e. equation (2)

2) Regular solution entropic approach ($S^E = 0$), i.e. equation (14)
3) Rigorous entropic approach, i.e. equation (12)

In cases 1) and 3) an expression for the enthalpy of mixing must be found, for which three options are possible:

i. Ideal, $\Delta H_{mix} = 0$
ii. Modelled, $\Delta H_{mix} = G^E = -RT\sum_i x_i \ln(\sum_j x_j \Lambda_{ij})$
iii. Measured, $\Delta H_{mix} = x_i(1-x_i)[a + bx_i + cx_i(1-x_i)]$

To predict the compositions the following expression is used:

$$x_i^l \gamma_i^l = x_i^s \gamma_i^s exp\left[\frac{\Delta H_{fus,i}}{RT_{m,i}}\left(\frac{T-T_{m,i}}{T}\right)\right] \quad (24)$$

Three progressively less ideal options can be used:

a. Ideal liquid phase, immiscible solid phase: $\gamma_i^l = 1$ & $x_i^s \gamma_i^s = 1$
b. Non-ideal liquid phase, immiscible solid phase: $\gamma_i^l \neq 1$ & $x_i^s \gamma_i^s = 1$
c. Non-ideal liquid phase, Non-ideal solid phase: $\gamma_i^l \neq 1$ & $\gamma_i^s \neq 1$

There are some restrictions on the ways in which the enthalpy of mixing estimates can be combined with the compositional estimates. For example: the assumption of ideal behaviour necessarily fixes both options resulting in only one possibility: (i) combined with (a).

The non-ideal behaviour of the temperature-composition dependence (b & c) can be calculated using either the modelled or measured enthalpies of mixing (ii & iii). For non-ideality in the liquid phase alone, it is possible to fit the Wilson parameters using only the eutectic temperature and composition. This is done by specifying the mole fraction of one component in the liquid phase, which in a binary fixes the other component. Equation (24) can be applied twice, once for each component, thus one is left with two equations and two unknowns.

For complex eutectic behaviour (both phases non-ideal) two expressions for the enthalpy of mixing are required to predict the compositions, one for the liquid phase and one for the solid phase. This would require two Wilson expressions and hence four model parameters. Despite the fact that equation (24) can be applied four times, an additional unknown remains, namely the solid phase mole fraction. If the eutectic composition is used, the same equations are generated for the solid and liquid phase. Thus a point other than the eutectic is required to perform the model parameter fit. This information is unlikely to be available when screening a wide variety of new mixture possibilities. For this reason the combination (ii & c) was not considered, leaving four combinations (i & a), (ii & b), (iii & b) and (iii & c). For reference these approaches are designated:

1) Ideal liquid, immiscible solid (i & a): IL, IMS
2a) Non-ideal liquid, immiscible solid, modelled ΔH_{mix} (ii & b): NIL, IMS, MOD
2b) Non-ideal liquid, immiscible solid, measured ΔH_{mix} (iii & b): NIL, IMS, MEA
3) Non-ideal liquid, Non-ideal solid, measured ΔH_{mix} (iii & c): NIL, NIS

These combinations are applied to each of the three enthalpy of fusion modelling approaches, i.e. 12 possibilities. However, since the enthalpic approach does not require the temperature-composition dependence, there is no distinction between options (iii & b) and (iii & c). Furthermore, the assumption of ideality means equation (12) is equivalent to (14) for this case (IL, IMS). Overall, that leaves 10 possible modelling combinations. By progressively considering the availability of data as well as the predictive performance for the temperature-composition dependence and enthalpy of fusion, the possibilities can be reduced as demonstrated in the following section.

Experimental data is utilised to validate the predictions for multiple systems: $NaNO_3$-KNO_3, $LiNO_3$-KNO_3 and $NaNO_3$-$LiNO_3$ across the entire range of composition. A combination of literature data [30-33] and experimentally determined DSC measurements (PerkinElmer DSC4000) are used. The measured data for 21 binary eutectics were found in literature [34]. In addition, the pure component properties for the 35 salts under consideration were also obtained from the same source [34] and are given in Table 1. The cost data was retrieved for reagent grade materials from the Sigma-Aldrich (Merck) online catalogue. For all salts the cost for supplying 500 g of material was used as this was the only amount at which prices for all the salts were available. These individual prices for the 35 salts used are also listed in Table 1.

Table 1: Salt properties and prices

Compound	Melting Point (ºC)	Enthalpy of Fusion (J/g)	Price ($/kg)
LiF	849	1041	661
LiCl	610	416	726
LiBr	550	203	204
LiI	469	44	4287
Li_2SO_4	858	84	210
$LiNO_3$	253	373	234
Li_2CO_3	732	509	280
NaF	996	794	563
NaCl	801	482	56
NaBr	742	255	522
NaI	661	158	355
Na_2SO_4	884	165	110
$NaNO_3$	307	177	133
Na_2CO_3	858	165	138
KF	858	507	378
KCl	771	353	53
KBr	734	215	134
KI	681	145	159
K_2SO_4	1069	212	87
KNO_3	335	88	121
K_2CO_3	900	202	126
MgF_2	1263	938	50
$MgCl_2$	714	454	167
$MgBr_2$	711	214	381
MgI_2	633	93	1187
$MgSO_4$	1137	122	156
$Mg(NO_3)_2$	426	275	3911
$MgCO_3$	990	698	423
CaF_2	1418	381	127
$CaCl_2$	772	253	512
$CaBr_2$	742	145	5020
CaI_2	783	142	4582
$CaSO_4$	1460	203	81
$Ca(NO_3)_2$	560	145	149
$CaCO_3$	1330	521	299

4. Results and discussion

4.1. Solution model influence on enthalpy of fusion estimates

Since the temperature-composition dependence is implicitly required for the enthalpy of fusion calculation using the entropic approach, it is considered first for the $NaNO_3$-KNO_3 combination. The most accurate result is predictably found using the least idealised approach, as demonstrated in Figure 4. This requires the use of expressions for the enthalpy of mixing for both the liquid [35] and solid [29] phase, in order to generate the activity coefficients via equation (22). The next best performer, in terms of the liquidus line, or initial freezing point, prediction is the Wilson model. However, this is not unexpected as the model parameters have been fit using the eutectic composition and temperature.

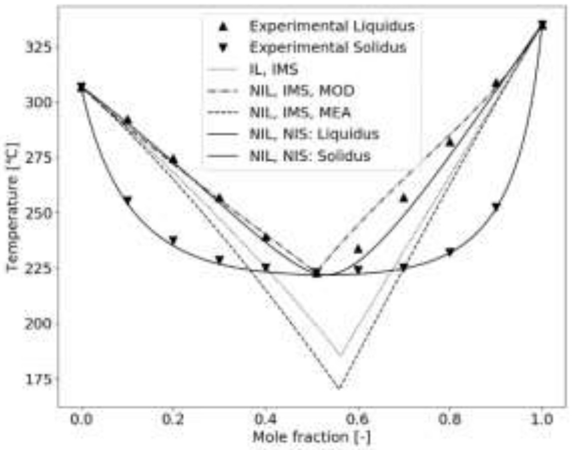

Fig. 4: Temperature-composition prediction ($NaNO_3$-KNO_3)

The least accurate result is found for the use of the experimentally determined enthalpy of mixing, combination (iii & b). Since the enthalpy of mixing is derived from purely liquid phase based measurements and not intended for application in situations of an immiscible solid phase, the result is perhaps not unsurprising. Due to the poor performance, this combination was excluded from the modelling possibilities. Since it can only be used in conjunction with the entropic approaches, this eliminates a further two options. The Schröder equation, based the assumption of ideality, performs only slightly better, however it requires only pure component properties.

These representations can now be used in conjunction with either the enthalpic or entropic approaches to determine the enthalpy of fusion for the mixture. However, significant variability is present in the available experimental data for enthalpy of fusion measurements. This is illustrated in Figure 5 for the $NaNO_3$-KNO_3 system. The cause of the spread is unclear and may be related to the cooling rate as discussed in the theory section. Nonetheless, it is important to combine these measurements in some way to obtain a representative baseline against which to rank model performance. One option would be to average the data. However, since the measurements have not all been conducted at the same compositions, this would require interpolation. Instead it was decided to fit a polynomial through the data which minimises the error w.r.t. to all available data points.

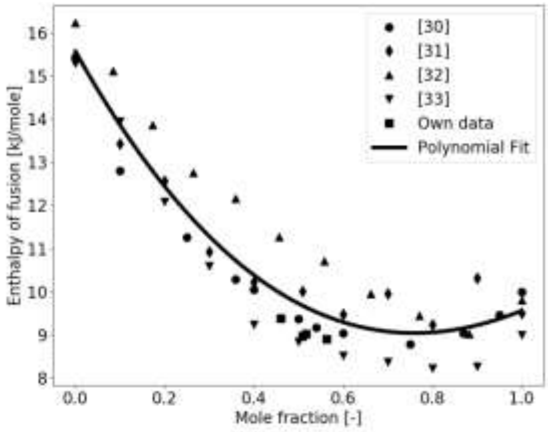

Fig. 5: Experimental enthalpy of fusion ($NaNO_3$-KNO_3)

Variation between datasets can be as high as ± 20%. The remaining eight modelling options can be compared to the representative fit of the experimental data. The liquid phase enthalpy of mixing is required in two of the three mentioned approaches and is a quantity which can be measured experimentally. The parameters of the Wilson model, Λ_{ij} and Λ_{ji}, have been fit using the eutectic composition and temperature as data points to give values of 0.329 and 0.984. These values agree well with those found by Davison and Sun [25] for the same system: 0.593 and 1.02. It is sensible to first compare the enthalpy of mixing predicted by the fitting of the Wilson model, using equation (15), to the measured values. The result is rather unexpected as shown in Figure 6, where the original, experimentally measured values and the expression given by Kleppa [35] are included.

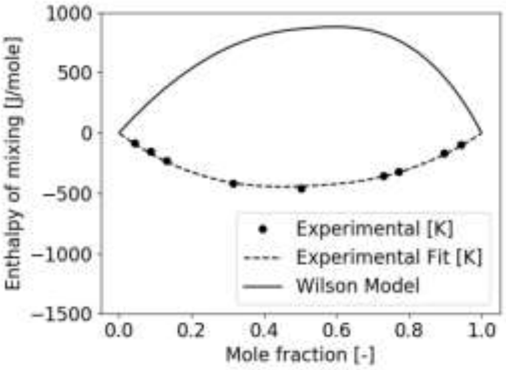

Fig. 6: Enthalpy of mixing in liquid phase ($NaNO_3$-KNO_3)

Not only is the value significantly larger than expected, it is has the opposite sign compared to the measured values. This demonstrates the risk when fitting a two parameter model solely based on the phase diagram. Despite providing a fairly accurate representation of the liquidus line, the approach is clearly invalid for calculating the enthalpy of mixing. Since the "regular solution entropic approach" does not contain the enthalpy of mixing, the Wilson equation can still be used in this case to represent the temperature-composition dependence. However, since the remaining two models, enthalpic and rigorous entropic, use ΔH_{mix} directly, these two combinations were also eliminated from consideration. The remaining four entropic based models, along with the two enthalpic ones, are considered in Figure 7.

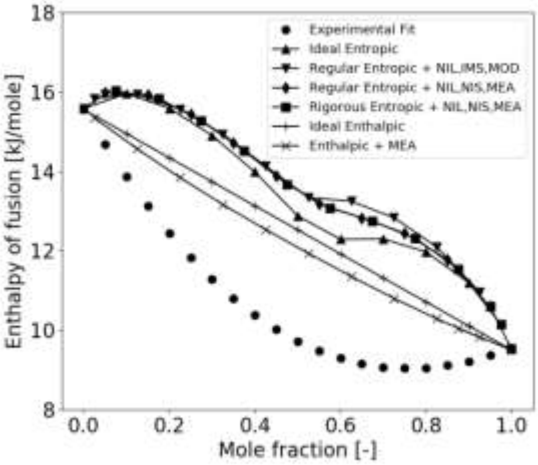

Fig. 7: Enthalpy of fusion prediction entropic approach ($NaNO_3$-KNO_3)

Overall the performance is very poor and the trend is opposite to expectations, based on experimental measurements. The figure demonstrates that in fact expression

(12) and (14) are identical, thus assuming the excess entropy of mixing is zero, has no impact in terms of the enthalpy of fusion. Furthermore, neither the assumption of ideality, nor the use of the Wilson equation significantly deteriorates the already unsatisfactory prediction. The Wilson equation very closely approximates the fully non-ideal behaviour in terms of the liquidus temperature-composition behaviour and as such does not deviate much from the full non-ideal descriptions. The figure also demonstrates that despite a fairly poor prediction of the phase diagram using the Schröder equation, the impact on the enthalpy of fusion prediction is comparatively low.

A slightly more accurate but equally disappointing estimate is found by using the enthalpic approach. The ideal enthalpic approach is simply a linear combination of the pure component enthalpies of fusion based on mole fraction. This is only marginally improved by the addition of the enthalpy of mixing (liquid phase). The reason for this is that the enthalpy of mixing is comparatively small, it amounts to less than 0.5 kJ/mole, as seen in Figure 6. Thus for this system it deviates very little from the ideal behaviour.

As pointed out in the derivation, the entropic approach is not theoretically sound at compositions other than the eutectic. The reason is the fact that everywhere else solidification involves multiple phases and occurs over a temperature range. Several attempts were made to correct for these phenomena by more accurately representing the behaviour as indicated in Figure 1. However, none of these corrections were able to reverse the direction of the deviation from positive (relative to ideal enthalpic mixing) to negative (observed experimentally). Ultimately the terms contributing to the expression were evaluated individually.

For the simplified entropic approach, equation (14) only has two terms, a temperature weighted average of the pure component properties and an entropic mixing term. The influence of each term was investigated and it was found that the poor fit arose from the fact that the entropic mixing term is multiplied by the mixture melting temperature. This greatly exaggerates its contribution. By implication materials with higher melting temperatures gain a higher contribution from the mixing entropy. This seems notionally inconsistent with the concept of entropy increase through mixing. It was found that if this term is omitted the prediction is significantly improved, as demonstrated in Figure 8. Using the idealised Schröder equation makes very little difference compared to the fully non-ideal temperature-composition dependence (Wilson omitted due to its similarity, to aid visualisation).

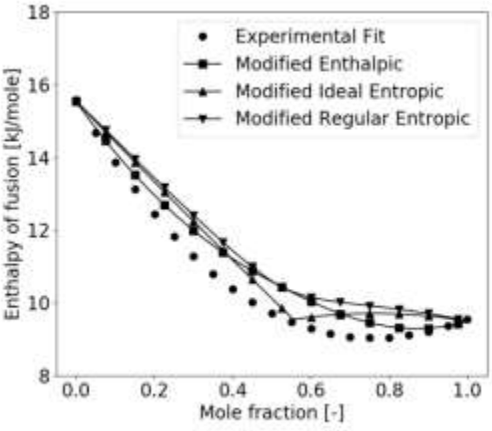

Fig. 8: Enthalpy of fusion prediction improvement ($NaNO_3$-KNO_3)

Clearly more work is still required to derive a fully consistent thermodynamic model which predicts fusion with high precision. Nonetheless, it was further found that subtracting the solid enthalpy of mixing term from the enthalpic approach also significantly improved the prediction. This term is supplied by Kramer and Wilson [29] through a fit of the full phase diagram. The solid enthalpy of mixing represents the reverse of the “unmixing” step proposed as part of the enthalpic derivation. Thus subtracting it from the liquid enthalpy of mixing is theoretically consistent. Initially it was thought that this contribution would be insignificant, however for the system under consideration this is clearly not the case. These four modified approaches provide adequate predictions for preliminary screening:

1) Modified enthalpic:

$$\Delta H_{fus,m} = \sum_i x_i \Delta H_{fus,i} + \Delta H_{mix,\ liquid} - \Delta H_{mix,\ solid} \quad (25)$$

2) Modified entropic:

$$\Delta H_{fus,m} = T_{m,mix} \sum_i x_i \left(\frac{\Delta H_{fus,i}}{T_{m,i}}\right) \quad (26)$$

   a) Temperature-composition using the Schröder equation
   b) Temperature-composition using the Wilson equation
   c) Temperature-composition using the enthalpy of mixing for both liquid and solid

Both the modified enthalpic and the third modified entropic approaches require expressions for the enthalpy of mixing for both liquid and solid. The former can be measured experimentally. As mentioned, the latter can only be obtained once the former has been measured, using a detailed phase diagram as the basis for fitting the remaining empirical expression [29]. This makes the approach impossible to apply to the screening of new components. However, once suitable components have been identified and fully characterised, these options will provide the most accurate estimate of the enthalpy of fusion as a function of composition. The use of the Wilson equation requires knowledge of the eutectic composition and temperature to obtain the model parameters, which is usually also unavailable for novel combinations. Thus the only practical option for preliminary property estimation is the modified entropic expression in conjunction with the Schröder equation which has thus far been proven to perform satisfactorily.

To ensure the conclusions reached do not exclusively apply to the $NaNO_3$-KNO_3 system, the modelling was also applied to two other nitrate systems: $LiNO_3$-KNO_3, $NaNO_3$-$LiNO_3$. For these systems the experimentally obtained enthalpy of mixing for liquids can be found in literature [27]. Furthermore the phase diagrams are freely available via the *FactSage* database [36]. Using this information it is possible to obtain the expression for the enthalpy of mixing in the solid phase, assuming a similar form to the liquid phase. The modelling results for the two systems, using all four modified models are shown in Figure 9 A and B.

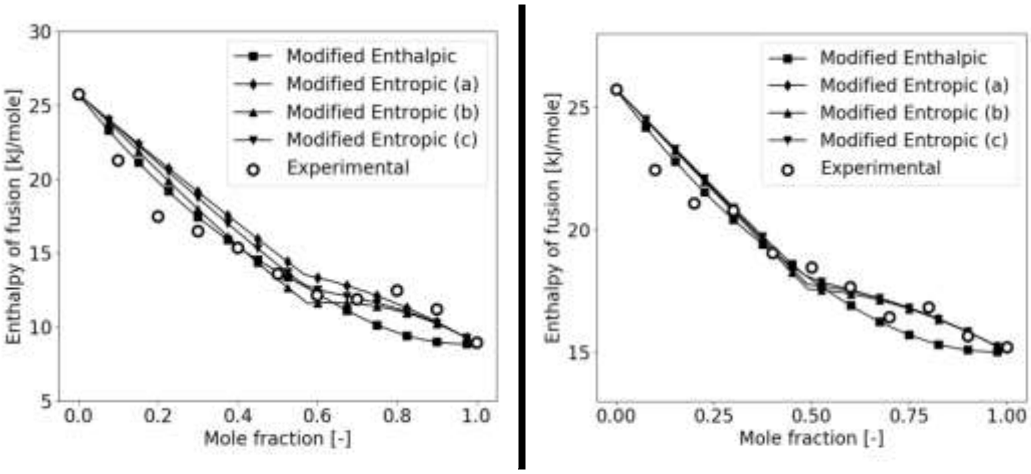

Fig. 9: Enthalpy of fusion prediction A) $LiNO_3$-KNO_3 B) $NaNO_3$-$LiNO_3$

In general the predictions are adequate and there is very little difference between the models. The entropic approaches seem to provide a slightly better representation of the data compared to the enthalpic. This demonstrates that the use of the Schröder equation in conjunction with the modified entropic equation should provide reasonable preliminary estimates for the enthalpy of fusion of nitrate salts. As wider validation of the approach, this model (2a) was used to predict the enthalpy of fusion for 21 binary eutectics found in literature [34]. The predicted results are compared to the actual values in Figure 10.

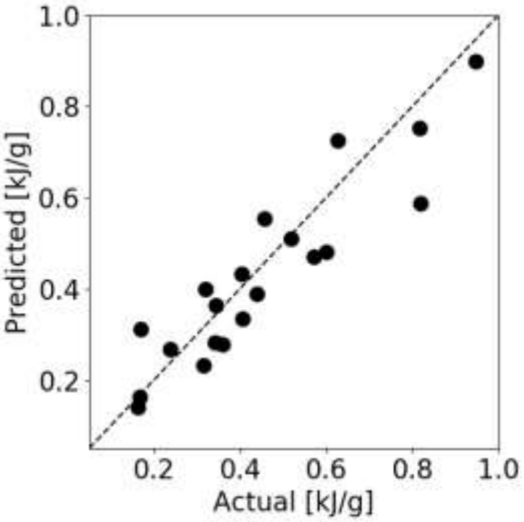

Fig. 10: Enthalpy of fusion prediction for 21 binary eutectics

The salts span a wide variety including halides, carbonates, sulphates and nitrates. The predictions agree well with the measured values and the uncertainty is close to the 20% deviation observed for different enthalpy of fusion measurements on the $NaNO_3$-KNO_3 system in Figure 5. The average root-mean-square (RMS) prediction error is 24.7%, calculated as $\sqrt{\{\sum(predicted\ value - measured\ value)^2\}/n}$ where n is the number of measurements. Individual errors are reported in Appendix A: Table A1. The presented approach requires only pure component properties, making it ideal for rapidly screening a wide selection of salts to explore all possible multicomponent combinations.

4.2. Pure component enthalpy of fusion estimation

In an effort to further extend the flexibility of the approach, the option of inferring the enthalpy of fusion was explored. This assumes that melting point data is easier to obtain than enthalpy of fusion data for potential, pure component candidates. In doing so, the search space of prospective mixtures could be greatly enlarged. An extensive list of enthalpies of fusion is available in the Yaws handbook of physical properties [37]. Additional values for ionic salts have also been reported by Kenisarin [34]. The values for all the elements in the Yaws list are plotted in Figure 11 against their melting temperature.

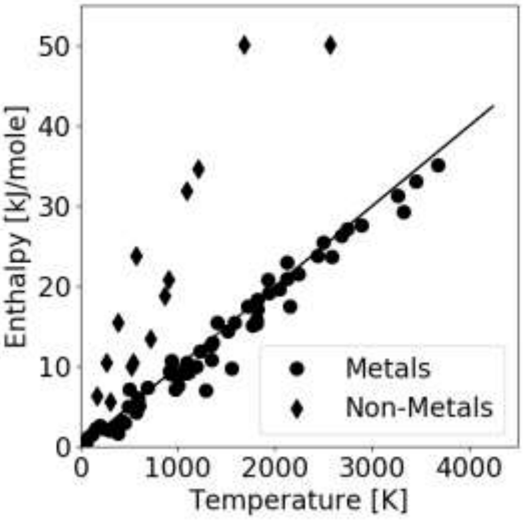

Fig. 11: Enthalpy of fusion vs melting point for elements

A distinction is made between metallic and non-metallic compounds. It is clear that the metallic compounds follow the trend indicated by the solid line (slope = 10 $J.mol^{-1}.K^{-1}$). This line represents the well-known “Richard’s Rule” [38], which states that the entropy of fusion is roughly constant at 7-14 $J.mol^{-1}.K^{-1}$. This is related to the enthalpy of fusion via equation (7). As pointed out by Nishizawa [39], non-metallic compounds tend to release more energy during melting since they have more ordered and complex crystalline structures than metals. This prompted a subdivision of the compounds in the list along a similar distinction, namely covalent and ionic compounds.

Here covalent compounds are crudely defined as being formed by combinations containing only non-metals, whereas ionic compounds contain both metallic and non-metallic constituents. The results for ionic compounds are displayed in Figure 12 along with the additional data from literature. In general the agreement is decent with a clear correlation being distinguishable. The trend line given in the figure has a slope of ~25 $J.mol^{-1}.K^{-1}$, which is a substantial increase compared to “Richard’s Rule” and in line with expectations for higher energy release in more complex, multicomponent, ionic crystals. The value is close to the number obtained by Redkin [40] for metal halide salts of 35 $J.mol^{-1}.K^{-1}$.

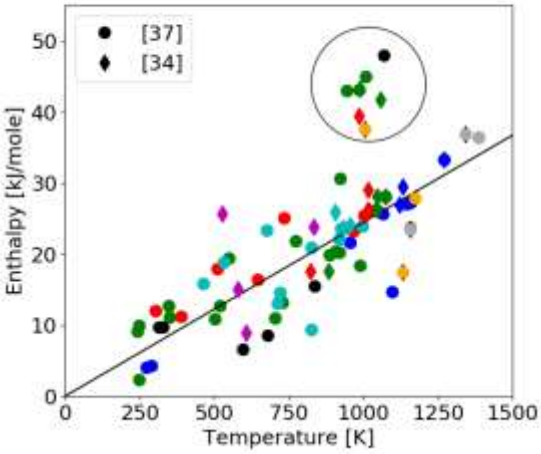

Fig. 12: Enthalpy of fusion vs melting point for ionic compounds (blue=fluorides, green=chlorides, red=bromides, cyan=iodides, magenta=nitrates, grey=sulphates, orange=carbonates)

There appears to be a group of exceptions, as indicated by the encircled region in Figure 12. This group predominantly contains divalent, metal halide salts. Also excluded from this figure are the ultra-high temperature metal oxides. Both of these groups exhibit exceptionally large enthalpies of fusion. Perhaps indicative of a more elaborate crystalline arrangement and higher bond strength, highlighting that the approach should be used with care in these cases. This also explains the slightly higher value found by Redkin [40]. The proposed enthalpy of fusion model (2a), using the Schröder equation, in conjunction with this correlation, only requires pure component melting point data. The impact of this on the predicted eutectic enthalpy of fusion is demonstrated in Figure 13.

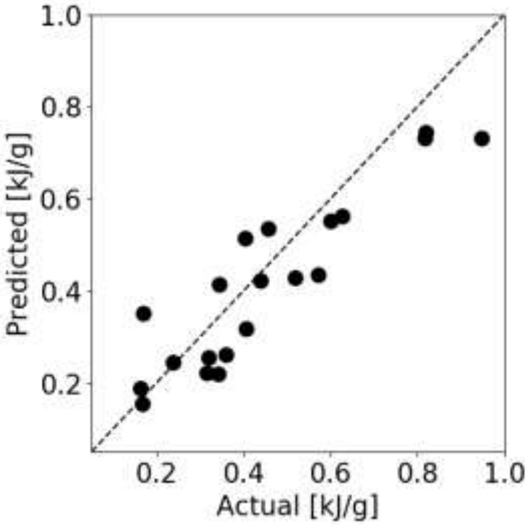

Fig. 13: Enthalpy of fusion prediction for 21 binary eutectics using melting point

The average RMS prediction error is marginally increased to RMS 30.6%. This is still close to the measurement uncertainty. Thus the correlation is simple and will provide a suitable first guess for compounds which only have melting point data available.

4.3. Cost optimisation

A preliminary screening has been done to identify the most attractive candidate combinations. In addition, this provides an initial indication of the lowest, achievable energy storage cost. The assessment considers four halide salts (F, Cl, Br and I) in addition to the nitrates, carbonates and sulphates of three alkali metals (Li, Na and K) and two alkali earth metals (Mg and Ca). As a sensible baseline for comparison it is useful to consider an existing industrial case study.

The Gemasolar plant has been operational since 2011 [41, 42]. The heliostat field based solar power plant uses a salt mixture close to the eutectic composition (60% $NaNO_3$ - 40% KNO_3) as storage medium. The plant has a storage capacity of around 15 hours with the salt being taken through a sensible temperature range of 290-565 ºC, well above the liquidus temperature of 238 ºC. At a heat capacity of around 1.5 $kJ.kg^{-1}.K^{-1}$ and at a cost of approximately \$128/kg (using Table 1) this represents an energy storage cost of ~0.31 \$/kJ.

From a pure component perspective, only six of the 35 chosen salts fall within this temperature range, at an average cost of 20 \$/kJ. Clearly a more economical and flexible option is needed and initially only eutectics were considered. This avoids any issues of incongruent melting and provides energy delivery at a constant temperature. All of the possible binary eutectic combinations using the 35 salts in Table 1 are represented in Figure 14, limited to those with a storage cost less than 20 \$/kJ. Numerous possibilities exist within a given temperature region.

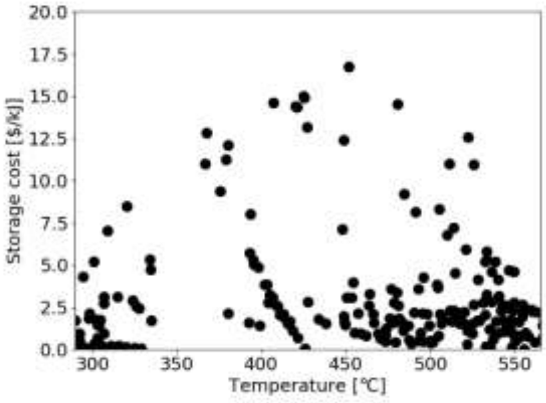

Fig. 14: Storage costs below 20 \$/kJ for binary eutectics

In order to reduce the number of possibilities the combinations may be grouped. If the given range of 290-565 ºC is subdivided into 5 ºC segments, it represents 55 sub-ranges. It is likely that multiple eutectics fall within the same sub-range, if this is the case, then the combination with the lowest storage cost is selected. For binary systems across the full range the cost is reduced to 7.99 \$/kJ and 50 of 55 sub-ranges are covered using 27 of the 35 potential salts. The models can easily be applied to higher order eutectics. However, further increases in the number of components leads to diminished returns as illustrated in Figure 15.

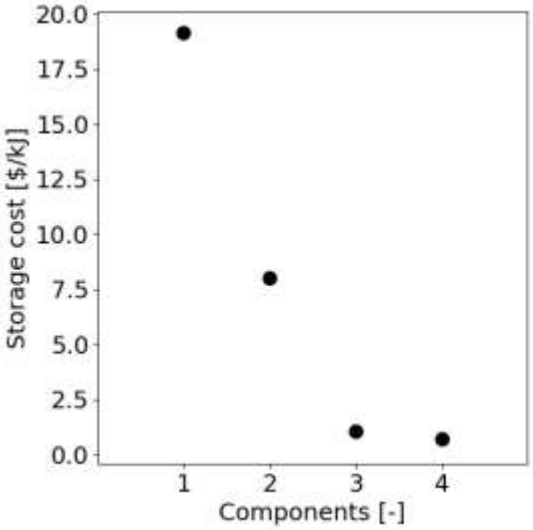

Fig. 15: Average storage cost over temperature sub-ranges as a function of the number of components (latent heat only)

Using ternary combinations the cost is further reduced to 1.06 $/kJ and all of the sub-ranges are covered using 26 of the 35 possible salts (salts excluded: LiI, $LiNO_3$, NaBr, NaI, $MgBr_2$, MgI_2, $CaCl_2$, $CaBr_2$, CaI_2). This brings the LHTES system cost to around three times the current sensible storage. It is possible to reduce the cost further to 0.71 $/kJ using quaternaries, however as can be seen from the figure, this only represents a small incremental benefit. Given the uncertainty associated with such complex systems, this is unlikely to be utilised in practice. Thus ternary systems seem to offer the optimal flexibility and economics to be of industrial value. The lowest cost in each of the sub-ranges achieved for ternary combinations are shown in Figure 16, but for a wider range than the operation of the Gemasolar plant.

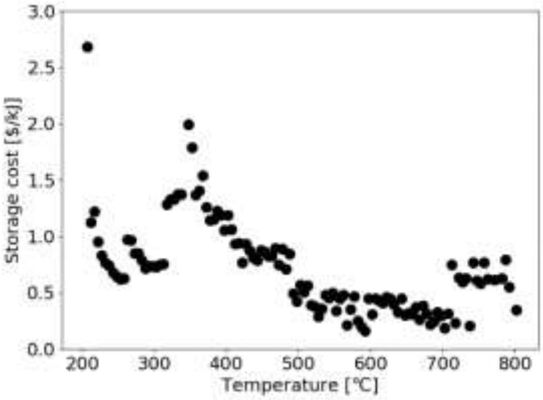

Fig. 16: Minimum storage cost for ternary combinations

The optimum combinations for each subrange are listed in Appendix A: Table A2. Beyond 350 ºC up to approximately 750 ºC there is a clear reduction in the storage cost with an increase in temperature. This is consistent with expectations from the modified “Richard’s Rule” proposed earlier, which indicates a rise in enthalpy of fusion with melting point. Assuming prices are more or less randomly distributed, this leads to a reduction in storage cost at higher temperatures. Thus future work to operate power plants at progressively higher temperatures will not only increase the efficiency of the power block but concurrently reduce the energy storage cost. The sudden increase in cost beyond 750 ºC is a result of the exclusion of KCl and NaCl from the available options. These materials have very low storage costs but since their melting points are in this region, they can only form eutectics at temperatures lower than this.

If the entire storage unit is operated around the melting point, in the region of the maximum Gemasolar temperature (565 ºC) the cost would be around 0.4 $/kJ. This is slightly higher than the current sensible storage value (0.31 $/kJ), but this is a conservative value. It is unlikely that the stored energy above and below the melting point would not also be utilised. This will depend on the operating procedures of these systems which are still being established. If the same size temperature range around the phase transition is also utilised for LHTES (heat capacities are similar) and assuming the two costs were in fact equal at 0.4 $/kJ, the store would achieve double the capacity at the same cost, i.e. 0.2 $/kJ. Since the sensible cost is actually 0.31 $/kJ the true estimate for combined latent and sensible storage is approximately 0.18 $/kJ.

An effort was made to reduce the current set of 26 salts which delivered the lowest possible cost. An optimisation was done to find the subset of eight candidate salts (selected from the full set of 35), which would result in the lowest cost while still covering a substantial temperature range. The operating region of the Gemasolar plant was chosen as the upper and lower limits (290-565 ºC). The optimal eutectic subset was found to be: LiBr, Li_2SO_4, Li_2CO_3, NaF, NaCl, KI, K_2SO_4 and $Ca(NO_3)_2$.

The average price achieved by this subset is 1.40 $/kJ, which still compares well to the value found for the full set of possibilities over the same range (1.06). The set manages to cover 73% of the selected temperature range. Thus future work will focus on the experimental exploration of these compounds and their binary/ternary eutectics. This will allow more accurate prediction of the achievable heat of fusion, phase behaviour and storage cost. Thereby enabling the development of eutectics tailored to specific application requirements in terms of melting behaviour and temperature.

Thus far only eutectic mixtures have been considered. If on the other hand incongruent melting is assumed to be manageable, the analysis can be repeated to include any potential composition. In this case only binaries were considered. Since the temperature range achievable with a single combination is greatly increased, the need for more than two components is largely negated. The enthalpy of fusion as a function of composition is calculated for all possible combinations using the Schröder equation and the modified entropic approach. For a given temperature interval all possible combinations yielding a mixture with a liquidus temperature in this range are considered. The composition is selected which minimises the energy storage cost.

An initial analysis indicated that the entire temperature range could be covered using a single eutectic: $LiNO_3$-KCl. Across the operating range the storage cost would decrease from 0.008 \$/kJ to 0.0045 \$/kJ at higher temperatures (more KCl) based on latent heat alone. Unfortunately this selection, while offering excellent economics, does have practical concerns. The eutectic composition is very close to pure $LiNO_3$. Thus if the system exhibits immiscible solid behaviour, as in Figure 1, a mixture with a composition closer to pure KCl would have to be cooled through the entire temperature range before completely solidifying (this additional energy has not been accounted for). Thus such a mixture will not be able to supply the bulk of its energy at constant temperature. This behaviour may be mitigated if the system exhibits terminal solid solutions with fairly close liquidus and solidus lines.

On the other hand, the exact operating mechanisms for LHTES systems have not yet been finalised, so for some designs a “semi-molten slurry” may prove an attractive option for heat exchange. This slurry would operate across the same temperature range as the current sensible store, but with significantly higher storage capacity. The next to optimal behaviour was found for a combination of the following salts: $LiNO_3$, $NaNO_3$, $Ca(NO_3)_2$, NaCl and KCl. This selection may be capable of delivering stored energy over a narrower range, however individual temperature regions and phase diagrams would have to be examined in detail. The achieved storage cost for these combinations are virtually equal to that of the prior, single binary.

It should be emphasised that this study has used the available pricing for fine chemicals, i.e. reagent grade materials. Industrial applications will most likely utilise bulk raw materials. While the properties of these materials will not be as good as the fine chemicals, indications are that their costs are up to three orders of magnitude less (see comparison to bulk values [43, 44] in Appendix A: Table A3). If a more conservative estimate of cost reduction by a factor of 100 is used, it means expected storage costs of eutectic LHTES systems should be approximately 1.8 $/MJ for a store operating temperature of around 550 ºC, with concomitant sensible energy recovery. However, given the ~25% uncertainty in the enthalpy measurements and their predictions, a value of 1.8 ± 0.45 $/MJ is more appropriate for cost estimates using bulk materials.

If issues such as incongruent melting associated with non-eutectic mixtures are overcome, LHTES cost using bulk materials could potentially be decreased to a very attractive 0.045 $/MJ. This number is conservative since it does not include the sensible energy released, which would depend on the operating range and the shape of the solidus line. Thus future work should focus on these “semi-molten slurry” options to establish the practical hurdles for implementation as they could dramatically decrease the overall storage cost.

5. Conclusions

Affordable energy storage is a key obstacle facing the widespread implementation of renewable options such as solar energy. Ionic salts and their eutectic mixtures have been identified as suitable candidates and are currently in use in industry as sensible storage options. However, in order to maximise the energy density and reduce the capital cost, it is necessary to consider other options such as the incorporation of latent heat. LHTES systems have been under investigation for some time; however no attempt has been made to screen the very large number of possibilities to identify the key candidates which represent the lowest cost per unit energy stored.

In order to achieve this, an adequate model for the enthalpy of fusion as a function of composition must be established. Three possible modelling approaches were considered: enthalpic, regular solution entropic and rigorous entropic. These approaches were combined with different methods of representing the enthalpy of mixing and the temperature-composition dependence. The temperature-composition dependence was not represented precisely using the assumption of ideality, however the impact of this on the predicted enthalpy of fusion was minimal. It was found that the use of a modelled excess Gibbs free energy may result in inconsistent predictions for the enthalpy of mixing.

None of the derived expressions could suitably represent the highly variable experimental data for the $NaNO_3$-KNO_3 system. However, it was discovered that modified versions of the theoretical expressions could significantly improve the predictions. By removing the entropic mixing term the entropic approach provided the best predictive capability across a wide range of binary systems. Additionally, by including a solid mixing term in the enthalpic approach, the accuracy was substantially improved. In the end it was found that the assumption of liquid phase ideality and solid phase immiscibility, combined with the modified entropic equation represented the best option for the initial screening of potential mixtures using only pure component properties. It was also demonstrated that the approach could be further generalised to using only pure component melting points via an adapted form of "Richard's Rule". Because of this relationship, it was also demonstrated that as the storage temperature is increased, storage cost should come down.

The approach was used to screen a wide variety of multicomponent, eutectic mixtures for application in the range 290-565 ºC. It was found that ternary mixtures provided a good trade-off between cost, flexibility and excessive complexity. Across the entire range an average price of 1.06 $/kJ was realised. For ternary mixtures the storage cost at a temperature of around 550 ºC (using only latent heat) was predicted to be around 0.4 $/kJ. If a similar operating temperature range to current sensible systems is assumed, the combination of sensible and latent storage could result in an overall cost of around 0.18 $/kJ, which is significantly better than current sensible storage using solar salt (~0.3 $/kJ).

In an effort to reduce the number of salts which should be pursued for detailed thermal studies in the future, an optimised subset of eight salts was found (LiBr, Li_2SO_4, Li_2CO_3, NaF, NaCl, KI, K_2SO_4 and $Ca(NO_3)_2$). These salts still achieve an average price of 1.40 $/kJ and cover 73% of the selected temperature range. Finally, non-eutectic mixtures were also considered as an alternative solution. These mixtures do pose significant practical hurdles which must be overcome, such as incongruent melting, a melting temperature range and the presence of multiple solid and liquid phases. However, if these can be mitigated, a single binary mixture, $LiNO_3$-KCl, can cover the entire temperature range at a storage cost of between 0.008 $/kJ to 0.0045 $/kJ.

The prices used in this study are based on fine chemicals, but if bulk materials are used it is likely that the storage cost for combined sensible and latent stores could be as low as 1.8 ± 0.45 $/MJ for a store operating temperature of around 550 ºC, taking into account measurement and prediction uncertainty. Future studies should explore the potential of non-eutectic, "semi-molten slurry" options since these could dramatically reduce the cost to lower than 0.045 $/MJ for bulk materials, if practical limitations can be overcome.

References

[1] Lund PD, Lindgren J, Mikkola J, Salpakari J. Review of energy system flexibility measures to enable high levels of variable renewable electricity. Renewable and Sustainable Energy Reviews. 2015 May 1;45:785-807.

[2] Gude VG. Energy storage for desalination processes powered by renewable energy and waste heat sources. Applied Energy. 2015 Jan 1;137:877-98.

[3] Krakowski V, Assoumou E, Mazauric V, Maïzi N. Reprint of Feasible path toward 40–100% renewable energy shares for power supply in France by 2050: A prospective analysis. Applied energy. 2016 Dec 15;184:1529-50.

[4] Fernández AG, Galleguillos H, Fuentealba E, Pérez FJ. Thermal characterization of HITEC molten salt for energy storage in solar linear concentrated technology. Journal of Thermal Analysis and Calorimetry. 2015 Oct 1;122(1):3-9.

[5] Relloso S, Lata J. Molten salt thermal storage: a proven solution to increase plant dispatchability. Experience in Gemasolar Tower plant. Proceeedings of SolarPaces. 2011 Sep:1-6.

[6] Khan J, Arsalan MH. Solar power technologies for sustainable electricity generation–A review. Renewable and Sustainable Energy Reviews. 2016 Mar 1;55:414-25.

[7] Desideri U, Campana PE. Analysis and comparison between a concentrating solar and a photovoltaic power plant. Applied Energy. 2014 Jan 1;113:422-33.

[8] National Renewable Energy Laboratory (US). Assessment of parabolic trough and power tower solar technology cost and performance forecasts. Vol. 550, no. 34440. DIANE Publishing, 2003.

[9] Badenhorst H. A novel heat exchanger concept for latent heat thermal energy storage in solar power towers: Modelling and performance comparison. Solar Energy. 2016 Nov 1;137:90-100.

[10] Tian Y, Zhao CY. A review of solar collectors and thermal energy storage in solar thermal applications. Applied energy. 2013 Apr 1;104:538-53.

[11] Farid MM, Khudhair AM, Razack SA, Al-Hallaj S. A review on phase change energy storage: materials and applications. Energy conversion and management. 2004 Jun 1;45(9-10):1597-615.

[12] Sharma A, Tyagi VV, Chen CR, Buddhi D. Review on thermal energy storage with phase change materials and applications. Renewable and Sustainable energy reviews. 2009 Feb 1;13(2):318-45.

[13] Zalba B, Marın JM, Cabeza LF, Mehling H. Review on thermal energy storage with phase change: materials, heat transfer analysis and applications. Applied thermal engineering. 2003 Feb 1;23(3):251-83.

[14] Gil A, Medrano M, Martorell I, Lázaro A, Dolado P, Zalba B, Cabeza LF. State of the art on high temperature thermal energy storage for power generation. Part 1—Concepts, materials and modellization. Renewable and Sustainable Energy Reviews. 2010 Jan 1;14(1):31-55.

[15] Raud R, Jacob R, Bruno F, Will G, Steinberg TA. A critical review of eutectic salt property prediction for latent heat energy storage systems. Renewable and Sustainable Energy Reviews. 2017 Apr 1;70:936-44.

[16] Janz GJ. Molten salts handbook. Elsevier; 2013 Jun 11.

[17] Fernández AG, Ushak S, Galleguillos H, Pérez FJ. Development of new molten salts with LiNO3 and Ca (NO3) 2 for energy storage in CSP plants. Applied Energy. 2014 Apr 15;119:131-40.

[18] Maeso MJ, Largo J. The phase diagrams of LiNO3-NaNO3 and LiNO3-KNO3: the behaviour of liquid mixtures. Thermochimica acta. 1993 Aug 28;223:145-56.

[19] Raud R, Bell S, Adams K, Lima R, Will G, Steinberg TA. Experimental verification of theoretically estimated composition and enthalpy of fusion of

eutectic salt mixtures. Solar Energy Materials and Solar Cells. 2018 Jan 31;174:515-22.

[20] Kosa L, Proks I, Strečko J, Adamkovičová K, Nerád I. Estimation of the heat of fusion of binary compounds and of eutectic using thermodynamic balances. Thermochimica acta. 1993 Dec 15;230:103-11.

[21] Smith, JM, van Ness HC, Abbott MM. Introduction to Chemical Engineering Thermodynamics. New York: McGraw-Hill, 1959, 5th edition.

[22] Walas SM. Phase equilibria in chemical engineering. Butterworth-Heinemann; 2013 Oct 22.

[23] DeHoff R. Thermodynamics in materials science. CRC Press; 2006 Mar 13.

[24] Misra AK, Whittenberger JD. Estimated heats of fusion of fluoride salt mixtures suitable for thermal energy storage applications.

[25] Davison SM, Sun AC. Thermodynamic analysis of solid–liquid phase equilibria of nitrate salts. Industrial & Engineering Chemistry Research. 2011 Oct 26;50(22):12617-25.

[26] Gmehling JG, Anderson TF, Prausnitz JM. Solid-liquid equilibria using UNIFAC. Industrial & Engineering Chemistry Fundamentals. 1978 Nov;17(4):269-73.

[27] Kleppa OJ, Hersh LS. Heats of mixing in liquid alkali nitrate systems. The Journal of Chemical Physics. 1961 Feb;34(2):351-8.

[28] Kleppa OJ. The solution chemistry of simple fused salts. Annual Review of Physical Chemistry. 1965 Oct;16(1):187-212.

[29] Kramer CM, Wilson CJ. The phase diagram of NaNO3—KNO3. Thermochimica Acta. 1980 Dec 30;42(3):253-64.

[30] Rogers DJ, Janz GJ. Melting-crystallization and pre-melting properties of NaNO3-KNO3.

[31] Benages-Vilau R, Calvet T, Cuevas-Diarte MA, Oonk HA. The NaNO3–KNO3 phase diagram. Phase Transitions. 2016 Jan 2;89(1):1-20.

[32] Xiao X, Zhang P, Li M. Thermal characterization of nitrates and nitrates/expanded graphite mixture phase change materials for solar energy storage. Energy conversion and management. 2013 Sep 1;73:86-94.

[33] Coscia K, Neti S, Oztekin A, Nelle S, Mohapatra S, Elliott T. The Thermophysical Properties of the NaNO3-KNO3, LiNO3-NaNO3, and LiNO3-

KNO3 Systems. InASME 2011 International Mechanical Engineering Congress and Exposition 2011 Jan 1 (pp. 889-894). American Society of Mechanical Engineers.

[34] Kenisarin MM. High-temperature phase change materials for thermal energy storage. Renewable and Sustainable Energy Reviews. 2010 Apr 1;14(3):955-70.

[35] Kleppa OJ. A new twin high-temperature reaction calorimeter. The heats of mixing in liquid sodium-potassium nitrates. The Journal of Physical Chemistry. 1960 Dec;64(12):1937-40.

[36] Bale CW, Chartrand P, Degterov SA, Eriksson G, Hack K, Mahfoud RB, Melançon J, Pelton AD, Petersen S. FactSage thermochemical software and databases. Calphad. 2002 Jun 1;26(2):189-228.

[37] Yaws CL. Chemical properties handbook. McGraw-Hill,; 1999.

[38] Richards JW. Relations between the Melting Points and the Latent Heats of Fusion of the Metals. Journal of the Franklin Institute. 1897;143(5):379.

[39] Nishizawa T. Thermodynamics of microstructures. Asm International; 2008.

[40] Redkin A, Korzun I, Reznitskikh O, Yaroslavtseva T, Zaikov Y, Kumkov S. Heat of fusion of halide salts and their eutectics. Journal of Thermal Analysis and Calorimetry. 2018 Feb 1;131(2):2021-6.

[41] Burgaleta JI, Arias S, Ramirez D. Gemasolar, the first tower thermosolar commercial plant with molten salt storage. SolarPACES, Granada, Spain. 2011 Sep 20:20-3.

[42] Relloso S, García E. Tower technology cost reduction approach after Gemasolar experience. Energy procedia. 2015 May 1;69:1660-6.

[43] Xu B, Li P, Chan C. Application of phase change materials for thermal energy storage in concentrated solar thermal power plants: a review to recent developments. Applied Energy. 2015 Dec 15;160:286-307.

[44] Liu M, Tay NS, Bell S, Belusko M, Jacob R, Will G, Saman W, Bruno F. Review on concentrating solar power plants and new developments in high temperature thermal energy storage technologies. Renewable and Sustainable Energy Reviews. 2016 Jan 1;53:1411-32.

Appendix A

Table A1: Binary eutectic prediction errors

Combination	**Error (%)**
KF-MgF_2	2
LiCl-$Ca(NO_3)_2$	2
$KN0_3$-$NaNO_3$	5
LiF-MgF_2	5
KF-LiCl	6
LiF-LiCl	7
LiF-NaF	8
NaCl-$CaCl_2$	11
KF-CaF_2	13
NaF-MgF_2	14
K_2C0_3-Na_2CO_3	16
LiF-KF	17
NaCl-$MgCl_2$	20
Li_2C0_3-K_2CO_3	21
NaF-NaCl	21
KF-KCl	22
NaF-CaF_2	25
NaF-NaBr	29
KF-KBr	35
LiF-CaF_2	39
LiF-MgF_2 (2)	42
LiCl-KCl	46

Table A2: Ternary salt eutectic combinations for each sub-range

Range [ºC]	Salt 1	Salt 2	Salt 3
205 - 210	LiCl	Li2SO4	KNO3
210 - 215	LiBr	Li2SO4	LiNO3
215 - 220	LiCl	Li2SO4	LiNO3
220 - 225	LiCl	LiBr	LiNO3
225 - 230	LiBr	LiNO3	Ca(NO3)2
230 - 235	LiBr	LiNO3	KBr
235 - 240	LiBr	LiNO3	NaCl
240 - 245	LiNO3	Na2CO3	KCl
245 - 250	LiNO3	NaCl	KBr
250 - 255	LiNO3	NaCl	KCl
255 - 260	LiNO3	MgF2	CaCO3
260 - 265	LiBr	NaNO3	MgCl2
265 - 270	NaNO3	KBr	Ca(NO3)2
270 - 275	NaNO3	Na2CO3	KCl
275 - 280	NaCl	NaNO3	Na2CO3
280 - 285	NaNO3	KCl	KBr
285 - 290	NaCl	NaNO3	KCl
290 - 295	NaNO3	KCl	MgCl2
295 - 300	NaNO3	KCl	MgF2
300 - 305	NaCl	NaNO3	MgF2
305 - 310	NaNO3	MgF2	MgCl2
310 - 315	NaNO3	MgF2	CaCO3
315 - 320	NaCl	KNO3	MgF2
320 - 325	K2SO4	KNO3	MgCl2
325 - 330	KNO3	MgF2	MgCl2
330 - 335	K2SO4	KNO3	MgF2
335 - 340	KNO3	MgF2	MgCO3
340 - 345	LiCl	Mg(NO3)2	Ca(NO3)2
345 - 350	LiBr	Li2SO4	KBr
350 - 355	LiCl	LiBr	Na2CO3
355 - 360	LiBr	Na2CO3	Ca(NO3)2
360 - 365	LiBr	KI	Ca(NO3)2
365 - 370	LiCl	LiBr	KCl
370 - 375	LiBr	KBr	Ca(NO3)2

375 - 380	LiBr	KCl	Ca(NO3)2
380 - 385	LiBr	NaCl	Ca(NO3)2
385 - 390	LiBr	Li2CO3	Ca(NO3)2
390 - 395	LiBr	MgCl2	Ca(NO3)2
395 - 400	LiBr	Na2CO3	KCl
400 - 405	LiBr	KCl	MgSO4
405 - 410	LiBr	NaCl	Na2CO3
410 - 415	LiBr	KCl	KBr
415 - 420	LiBr	NaCl	KBr
420 - 425	LiBr	NaCl	KCl
425 - 430	LiF	LiBr	KCl
430 - 435	LiBr	Li2CO3	KCl
435 - 440	LiBr	KCl	MgCl2
440 - 445	NaCl	KCl	Ca(NO3)2
445 - 450	LiBr	KCl	CaSO4
450 - 455	LiBr	KCl	K2SO4
455 - 460	KCl	MgCl2	Ca(NO3)2
460 - 465	NaCl	MgCl2	Ca(NO3)2
465 - 470	KCl	CaSO4	Ca(NO3)2
470 - 475	Na2CO3	KCl	KBr
475 - 480	NaCl	K2SO4	Ca(NO3)2
480 - 485	NaCl	KCl	KI
485 - 490	Li2CO3	KCl	KI
490 - 495	NaCl	Na2CO3	KCl
495 - 500	NaCl	KCl	KBr
500 - 505	Na2CO3	KCl	MgCl2
505 - 510	KCl	KBr	MgCl2
510 - 515	NaCl	Na2CO3	MgCl2
515 - 520	NaCl	Na2SO4	KCl
520 - 525	Li2CO3	NaCl	KCl
525 - 530	NaCl	KCl	MgCl2
530 - 535	NaCl	KCl	K2CO3
535 - 540	NaCl	Na2SO4	MgCl2
540 - 545	Li2CO3	NaCl	MgCl2
545 - 550	NaCl	KF	MgCl2
550 - 555	NaF	NaCl	KCl
555 - 560	NaF	KCl	MgCl2
560 - 565	KCl	KBr	MgF2
565 - 570	NaCl	KCl	CaF2
570 - 575	KCl	MgCl2	CaF2
575 - 580	NaCl	KBr	MgF2

580 - 585	NaCl	KCl	MgCO3
585 - 590	NaCl	KCl	CaCO3
590 - 595	NaCl	KCl	MgF2
595 - 600	Na2SO4	KCl	MgF2
600 - 605	NaCl	MgF2	MgCl2
605 - 610	NaCl	K2CO3	CaF2
610 - 615	NaCl	Na2SO4	MgF2
615 - 620	KCl	K2CO3	MgF2
620 - 625	NaF	KCl	CaF2
625 - 630	NaCl	K2CO3	CaCO3
630 - 635	NaCl	K2CO3	MgF2
635 - 640	KCl	K2SO4	CaF2
640 - 645	K2SO4	MgCl2	CaF2
645 - 650	KCl	CaF2	CaSO4
650 - 655	NaCl	K2SO4	CaSO4
655 - 660	NaCl	K2SO4	CaF2
660 - 665	KCl	MgCO3	CaF2
665 - 670	KCl	K2SO4	MgF2
670 - 675	MgF2	MgCl2	CaF2
675 - 680	KCl	CaSO4	CaCO3
680 - 685	KCl	MgF2	CaF2
685 - 690	NaCl	K2SO4	MgF2
690 - 695	KCl	MgF2	MgCO3
695 - 700	NaCl	CaSO4	CaCO3
700 - 705	NaCl	MgF2	CaF2
705 - 710	NaCl	MgF2	MgCO3
710 - 715	K2CO3	MgCO3	CaSO4
715 - 720	KCl	MgF2	CaCO3
720 - 725	LiF	MgF2	CaSO4
725 - 730	K2SO4	K2CO3	MgF2
730 - 735	Na2SO4	MgF2	CaF2
735 - 740	NaCl	MgF2	CaCO3
740 - 745	Na2CO3	MgF2	CaCO3
745 - 750	K2CO3	MgF2	CaSO4
750 - 755	K2CO3	MgF2	CaF2
755 - 760	NaF	CaF2	CaSO4
760 - 765	LiF	MgF2	CaCO3
770 - 775	NaF	K2SO4	MgF2
780 - 785	K2SO4	MgCO3	CaF2
785 - 790	NaF	MgCO3	CaCO3
790 - 795	K2SO4	CaF2	CaSO4

800 - 805	MgF2	CaF2	CaSO4

Table A3: Comparison of bulk and fine chemical prices

	Fine ($/kg) (Merck)	Bulk ($/kg) [43, 44]	Ratio
LiCl	726	7.8	93
Li_2CO_3	280	6.355	44
NaF	563	0.05	11263
NaCl	56	0.085	654
$NaNO_3$	133	0.38	350
Na_2CO_3	138	0.17	809
KF	378	0.1	3781
KCl	53	0.31	170
KNO_3	121	0.85	142
K_2CO_3	126	1.05	120
MgF_2	50	0.01	5023
$MgCl_2$	167	0.275	606
CaF_2	127	0.5	255
$CaCl_2$	512	0.14	3656
$Ca(NO_3)_2$	149	0.25	598

Average price increase ratio bulk to fine chemical = 1838

Where multiple values are given for the same chemical the average value is used.